

Chapter-III

Studies On Magnetisation
And Permeability

CHAPTER - III

STUDIES ON MAGNETISATION AND PERMEABILITY.

3.1 INTRODUCTION :

In the ferrites, magnetisation is the net result of antiparallel magnetic moment of the cations. One of the most striking properties of a magnetic material is its spontaneous magnetisation (M_s). For many applications of magnetic material such as in transformer or inductance, a high value of ' M_s ' is required. For microwave applications a material with a low value of ' M_s ' is required. The value of ' M_s ' depends on following factors.

- i) The magnitude of the atomic magnetic moments and the number of these ions per unit volume.
- ii) The magnetic ordering temperature or Curie temperature.

In ferrites, the study of hysteresis gives valuable data on saturation magnetisation M_s , permeability, μ , coercive force ' H_c ', and remanance ratio (M_r/M_s). Therefore the magnetic parameters related to hysteresis decide the nature of application of ferrites. The value of permeability with wide range makes suitable for various frequency range application. So that, the ferrites can be suitably used in different frequency applications. The ferrites can be classified into two groups on the basis of coercive force ' H_c '. Ferrites with low coercive force are called soft ferrites and with high coercive force are called hard ferrites.

The soft ferrites are used in the manufacture of core of transformer, motors and generator, high frequency inductance, low coercive force and small hysteresis losses. Hard ferrites are generally used as permanent magnet.

According to Neel¹ (1949) the coercive force 'H_c' is related with saturation magnetisation, the internal stresses, porosity² and anisotropy³. Hysteresis properties are highly sensitive to crystal structure, heat treatment, chemical constitution, porosity and grain size⁴ etc.

The saturation magnetisation is basic property of ferrites which can be measured by ballistic method⁵, the vibrating coil magnetometer^{6,7}, vibrating sample magnetometer^{8,9} and microwave methods^{10,11}. A brief discussion on the hysteresis, Curie temperature, permeability is presented in this chapter.

3.2 THEORETICAL ASPECTS :

A demagnetised ferromagnetic material shows a state of zero magnetisation. The phenomenon of spontaneous magnetisation was first explained by Weiss¹² (1907) by postulating the existence of molecular field. He suggested that the magnetic material contains large number of regions in which spins are aligned.

According to Barkhausen¹³ the change in magnetisation in applied field which supports the interpretation of rotation of

magnetisation of the domains. Landau and Lifshitz showed that the domain formation in any ferromagnetic material is a consequence of considerable reduction in magnetostatic energy from the saturation magnetisation. Heisenberg¹³ (1928) gave the theory to overcome the limitations of Weiss molecular field theory and put forth the quantum mechanical treatment of exchange interaction between the uncompensated spins of electrons in the partially filled 3-d shell. According to Heisenberg under certain conditions the exchange energy produces effects similar to those of Weiss molecular field. In this case electrons with parallel spins have lower energy than those with antiparallel alignments.

Spontaneous magnetisation can also be arises as a result of negative exchange interaction under favourable conditions. According to Neel¹ (1949) the neighbouring magnetic moments are antiparallel. This is the origin of spontaneous magnetisation in ferrites, where the magnetic moments are arranged in antiparallel fashion. The magnetic moment associated to the magnetisation is mainly due to spin magnetic moments. However, the non-integral values in case of Fe, Ni, Co at 0°K could not be explained by Heisenberg model.¹⁴ The explanation of this has been based on band theory of solids (Stoner 1933).¹⁵ The exchange energy is given by,

$$W_{ex} = 2JS^2 \sum_{i \neq j} \cos \phi_{ij} \quad \dots\dots(3.1)$$

where S = total spin momentum per atom

θ_{ij} = the angle between spin momentum vector of atom i and j .

Neel developed the theory of antiferromagnetism and ferrimagnetism on the basis of two sub-lattice model which was proved experimentally¹⁶ first by Gorter (1950) and by Guillaud (1949,50,51). Neel theory had been extended by Yafet and Kittle¹⁷ by assuming triangular spin arrangement, in which A-A and B-B interaction are comparable in magnitude to the A-B interaction.

3.3 MAGNETIC ANISOTROPY :

The term anisotropy is generally referred to describe directional dependence of some physical properties like elasticity and strength, which are dependent on crystallographic directions. The term anisotropy energy is the difference between the energy required to magnetise the samples to saturate along the hard direction and that required along an easy direction. Ferrites are cubic crystals, the anisotropy energy is given by ,

$$W_k = K_1(\alpha_1^2\alpha_2^2 + \alpha_2^2\alpha_3^2 + \alpha_3^2\alpha_1^2) + K_2\alpha_1^2\alpha_2^2\alpha_3^2 + \dots \quad \dots (3.2)$$

where K_1 and K_2 are anisotropy constant and $\alpha_1\alpha_2\alpha_3$ are the direction cosines of magnetisation vectors with respect to cubic axis.

This energy is important in explaining the properties of magnetic materials such as permeability and coercive force.

The constant K_1 and K_2 changes from material to material and

are temperature dependent. They are also vary with structure and nature of magnetic ion. The electronic structure of magnetic ion contributes to anisotropy¹⁸. The influence of the temperature variation of 'Ms' on that of 'K' was first predicted by Zener.¹⁹ He showed that the anisotropy constant 'K' decreases much faster with increasing 'T' than does saturation magnetisation 'Ms'.

For the bulk magnetisation, the anisotropy energy is given by,

$$W_k = K_1 \sin^2 \theta \quad \dots\dots(3.3)$$

where K_1 = is the anisotropy constant

θ = is the angle between L and S.

When the crystal is strained, there is change in anisotropy energy, which is called as magneto-elastic energy ($W \lambda$). It is due to change in interatomic spacing. The magnetostatic energy (W_m) is the work required to assemble all the dipoles constituting the body which occurs as a result of division of crystal into domains. Bloch²⁰ (1932) has shown that the change in the magnetisation between two neighbouring domains takes place over a finite width. This wall of finite width contains spins whose orientations gradually changes from one domain to other domain. The thickness of domain wall is determined by the condition of minimum total energy. It is given by,

$$\sigma = (A/K)^{1/2} \quad \dots\dots(3.4)$$

This leads to the wall energy

$$W_r = 4/(AK)^{1/2} \quad \dots\dots(3.5)$$

where A = is exchange energy constant.

and K = anisotropy constant

In principle, the optimum domain configuration can be determined from the condition of minimum free energy such as ,

$$W = W_{ex} + W_k + W\lambda + W_m + W_r \quad \dots\dots(3.6)$$

for particular value of applied field.

3.4 MAGNETOSTRICTION :

Ferrites exhibits magnetostriction, where in dimensional changes are associated with magnetisation due to lowering of anisotropy energy by the determination of crystal lattice. Magnetostriction also gives rise to an induced strain anisotropy when stress is applied to the crystal.

The dimensional change of the crystal as a function of magnetisation is known as magnetostriction. The increase in crystal energy due to interaction of magnetisation and the strain of the crystal, which is generally depends on the direction of magnetisation and the crystalline axis is known as magneto-crystalline energy. Due to magnetostriction, effective anisotropy energy changes. Most of the ferrites exhibit negative incremental change except for few cases like FeFe_2O_4 .

3.5 HYSTERESIS AND MAGNETIC DOMAIN :

Weiss suggested that the specimen is composed of smaller regions which are magnetised and are randomly oriented with respect to each other would lead to zero magnetisation. These tiny regions are known as magnetic domains. The net magnetisation exhibited in the presence of small applied magnetic field is a consequence of orientation of direction of component of each magnetic domain in the direction of applied field. The domain formation is a consequence of the process which minimises the magnetic energy of the system. They are exchange energy, anisotropic energy, magnetostriction energy and magnetostatic energy. The change in the direction of antiparallel spin in the neighbouring domains takes place via domain wall having thickness of few hundred of interatomic distance.

3.6 MAGNETISATION CURVE AND HYSTERESIS :

The hysteresis or irreversibility is a phenomenon observed in ferro or ferri-magnetic material in which after saturation a decrease in 'H' to zero does not reduce 'M' to zero. The variation of 'M' to 'H' determines susceptibility ($\chi = M/H$), whereas B-H curves determine permeability ($\mu = B/H$) shown in Fig. 3.1

Generally an irreversibility and hysteresis in ferromagnetic material are attributed to impediment to the motion of domain wall. The impediments are due to grain boundaries, inclusions²¹ and heterogeneities due to other phases. Magnetisation increases slowly by irreversible wall motion at low field, then magnetisation increases

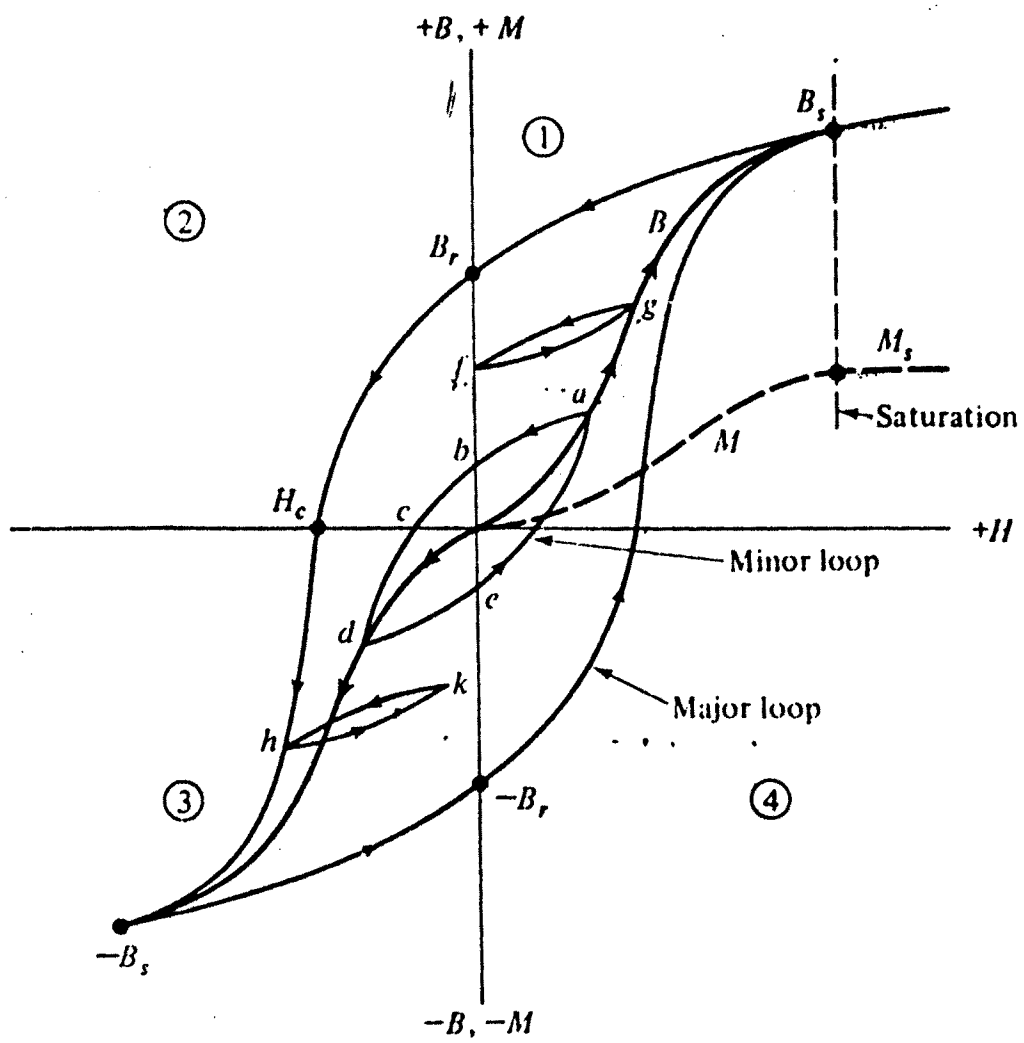


Fig. 3-1 3-1

above critical field by irreversible wall motion; also it increases at very high field by irreversible rotation. Above the threshold field, Barkhausen jumps are observed in magnetisation when the wall energy is maximum. This leads to irreversible increase in magnetostatic and magnetoelastic energies of the material under the action of external magnetic field. During magnetisation reversal nucleation has to proceed before the sequence of reversible and irreversible wall motion and spin rotation can take place. A model of wall motion was proposed by Keroten²² (1943) for an inhomogeneous material, having non magnetic inclusion, the changes in the energy of domain wall is due to variation of the area of the wall.

The strain and the inclusion theories considered only plane domain walls and regular arrays of imperfection. Further work on the problem led Neel to establish the variations in the magnitude and direction of the magnetisation. From this theory Neel calculated critical field required for irreversible moments of domain wall and coercivity.

3.7 PERMEABILITY :

The initial permeability is a sensitive function of the microstructure. To achieve high permeability the microstructure has to be controlled. In magnetic material the property of permeability is important which is related to microstructure, grain diameter, grain boundary etc. The initial permeability (μ_i) is the small signal value of permeability. Its value relative to that of vacuum is given by,

$$\mu_i = 1/\mu_0 \lim_{H \rightarrow 0} B'/H \quad \dots(3.7)$$

where μ_0 is the magnetic constant = $4\pi \times 10^{-7}$ B and H are in tesla and Am^{-1} respectively. Because of loss mechanism cause a phase difference between 'B' and 'H'. The initial permeability (μ_i) is complex and may be expressed in its real (inductive) and imaginary (loss) components.

$$\mu_i = \mu'_s - j\mu''_s \quad \dots\dots(3.8)$$

where μ'_s and μ''_s are real and imaginary components respectively.

Measurements of complex permeability of ferro and ferrimagnetic materials are often carried out at different points on the hysteresis loop with an audio-frequency magnetic field of small amplitude on the magnetising field. Previous workers^{23,24} shown that one can get a larger permeability when a given hysteresis loop point is reached by magnetising field, which varies with time. Improved permeability under such 'dynamic' conditions have been found with magnetic field and test field e.g. by the application of cyclic elastic stresses²⁵ or by rapid variation of temperature.²⁶

The temperature factor ' α_F ' is defined by the following relations,

$$\alpha_F = \mu_2 - \mu_1 / \mu_1 \mu_2 (\theta_2 - \theta_1) \quad \dots\dots(3.9)$$

where μ_1 and μ_2 are permeabilities measured at temperature θ_1 and θ_2 respectively. The permeability normally taken to be real part of the initial permeability. Later Schlemann^{27,28} presented the formula for the permeability in the completely demagnetised state.

3.8 LOSSES :

The important mechanism of losses are (a) Hysteresis loss
 b) Eddy current loss (c) permeability loss (d) Residual loss (e)
 wall resonance loss. For ferrites working at low fields, the
 hysteresis and eddy current losses are relatively small and major
 contribution comes from the remaining sources.

3.8 (a) HYSTERESIS LOSS :

The energy 'dE' required to change magnetisation M to M.dM
 at a field 'H' is given by,

$$dE = HdM \quad \dots\dots(3.10)$$

Thus the total ^{energy} absorbed for a complete hysteresis cycle is,

$$W = \oint HdM \quad \dots\dots(3.11)$$

which is equal to the area under the hysteresis loop. Low coercivity
 or high permeability results in a small area under the loop and hence
 a low loss, which is hysteresis loss. The hysteresis loss is due
 to irreversible domain wall displacement.

3.8 (b) EDDY CURRENT LOSS :

An electric current is induced in the magnetic core material
 by an alternating magnetic field. This causes heating and power loss.
 It is found that the power loss per second is proportional to AF^2/ρ

where F = is frequency and

ρ = is electrical resistivity of the core
 material.

Technically applied cores, the corresponding eddy current losses are given approximately by ,

$$\frac{(\tan\delta)_{\text{eddy}}}{\mu} \approx = (2 \times 10^{-5})F \quad \dots\dots(3.12)$$

where F is frequency in mega-hertz (MHz).

3.8 (c) PERMEABILITY LOSS :

When a magnetic material is used in an alternating magnetic field a certain portion of the magnetic energy is absorbed by material and dissipated as heat. In an alternating field we have,

$$H = H_0 \exp (i\omega t) \quad \dots\dots(3.13)$$

then the induction B, can in general be expressed as,

$$B = B_0 \exp i (\omega t + \delta) \quad \dots\dots(3.14)$$

so that,

$$\begin{aligned} \mu &= B/H \\ &= B_0/H_0 (\cos \delta + i \sin \delta) \\ &= \mu' + i\mu'' \quad \dots\dots(3.15) \end{aligned}$$

where μ' gives that the component of flux which is in phase and μ'' is out of phase with the applied field. The energy loss per cycle can be shown proportional to μ'' .

The ratio $\mu''/\mu' = \tan \delta$ is called as power factor or loss factor.

The quality factor ' Q ' is defined as ,

$$Q = \mu' / \mu'' = 1 / \tan \delta \quad \dots\dots(3.16)$$

3.8 (d) RESIDUAL LOSS FACTOR :

It has been noted that the phase difference between sinusoidal 'B' and 'H' in a ferrite core tends at vanishingly small amplitudes to a finite value called as residual loss angle ' δ_r '. This is often expressed as a residual loss tangent, ($\tan \delta_r$).

$$\tan \delta_r = \mu''_s / \mu'_s \quad \dots\dots(3.17)$$

where μ''_s and μ'_s are imaginary and real components of permeability.

It is convenient in the application of ferrite to inductors to use this quantity normalised with respect to the initial permeability, that is , $\tan \delta_r / \mu_i$

This is called as residual loss factor.

3.8 (e) WALL RESONANCE LOSS :

In certain samples, the low frequency loss has been identified due to domain wall resonance. If the domain wall is distributed from its equilibrium position, a restoring force sets in which tries to bring it back. The wall like a stretched membrane has natural frequency of oscillation. If the frequency of applied magnetic field matches this natural frequency, resonance absorption sets in.

3.9 DISACCOMMODATION FACTOR :

When a magnetic material is subjected to a transitory disturbance, which may be of mechanical, magnetic or thermal origin, the pattern of domains is disturbed and they do not return to their original position. In those regions of the material where the direction of spontaneous magnetisation has changed. This results in an increasing anisotropy, so the wall mobility is reduced and observed permeability falls. For the purpose of specification a standard disturbance is usually adopted. This consists of the application of an alternating field of sufficient strength to saturate the material and then the reduction of the amplitude smoothly to zero. The initial permeability is measured at low time intervals after the cessation of the disturbance.

The dissaccommodation factor is defined as²⁹,

$$DF = (\mu_1 - \mu_2) \mu_1^{2 \log_{10}(t_2 - t_1)} \quad \dots\dots(3.18)$$

where μ_1 and μ_2 are initial permeabilities measured at times ' t_1 ' and ' t_2 ' respectively after the disturbance.

3.10 EXPERIMENTS :

3.10 (a) CURIE TEMPERATURE MEASUREMENTS :

The experimental set up used for the measurement of Curie temperature is as shown in Fig. 3.2.

The electromagnet and the soft iron piece are insulated from

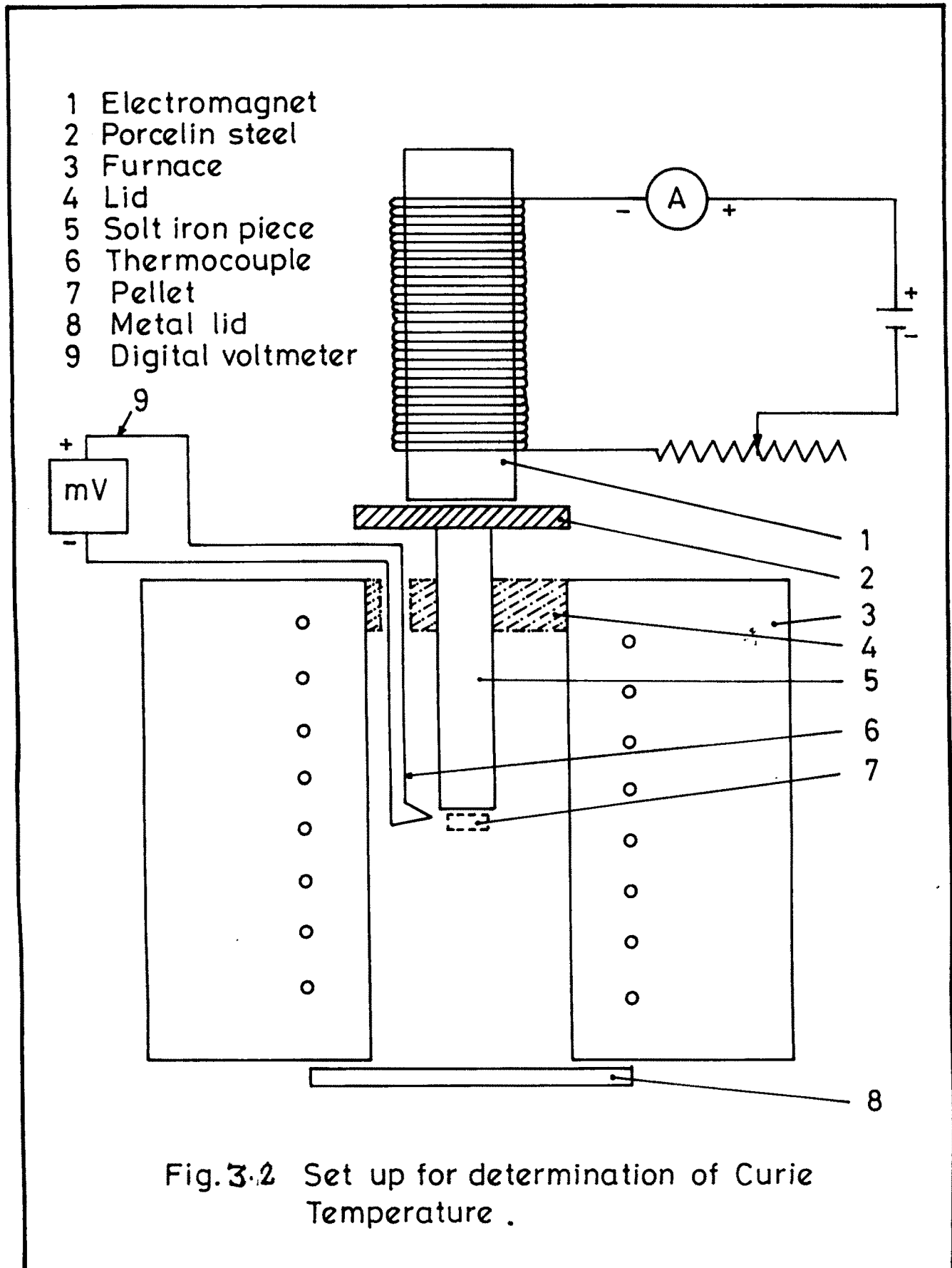


Fig. 3.2 Set up for determination of Curie Temperature .

each other. The porcelain sheet is used for this purpose. The magnetism was induced in the soft iron piece placed inside the furnace. The sample was fixed to this soft iron piece by raising the position of the sample through the aperture at the base of the furnace. The phenomena of attraction between the magnet and the sample helps the fixation of the sample to the soft iron piece. This was ensured by the use of mirror. At the bottom of the furnace, a bed of cotton wool was placed so as to avoid the breaking of the pellet when it falls. The calibrated chromel-Alumel thermocouple was introduced in the furnace to measure the temperature of it as shown in Fig. 3.2.

The temperature of the furnace was then raised slowly with the help of dimmerstat. At particular temperature the pellet detached from the electromagnet, and the millivoltmeter reading was noted. With the help of calibration chart the temperature corresponding to the millivolt is determined as a Curie temperature. The procedure is repeated for different samples. The Curie temperature of the series $\text{Cd}_{0.3} \text{Ni}_{0.7+t} \text{Mn}_t \text{Fe}_{2-2t} \text{O}_4$ with the variation of 't' (t=0 to 0.4) as shown in Table 3.1.

From the Table it is observed that, by the addition of 'Mn', Curie temperature decreases.

TABLE 3.1
VALUES OF T_c FROM EXPERIMENTS

Composition	Curie Temperature from T _c (°K)		
	Experimental	Conductivity	Permeability
$\text{Cd}_{0.3}\text{Ni}_{0.7}\text{Fe}_2\text{O}_4$	801	800	785
$\text{Cd}_{0.3}\text{Ni}_{0.75}\text{Mn}_{0.05}\text{Fe}_{1.9}\text{O}_4$	766.0	769.2	775.0
$\text{Cd}_{0.3}\text{Ni}_{0.8}\text{Mn}_{0.1}\text{Fe}_{1.8}\text{O}_4$	745.4	740.7	712.5
$\text{Cd}_{0.3}\text{Ni}_{0.85}\text{Mn}_{0.15}\text{Fe}_{1.7}\text{O}_4$	725.3	724.6	690.5
$\text{Cd}_{0.3}\text{Ni}_{0.9}\text{Mn}_{0.2}\text{Fe}_{1.6}\text{O}_4$	701.5	714.2	710.0
$\text{Cd}_{0.3}\text{Ni}_{1.0}\text{Mn}_{0.3}\text{Fe}_{1.4}\text{O}_4$	689.0	666.6	675.0
$\text{Cd}_{0.3}\text{Ni}_{1.1}\text{Mn}_{0.4}\text{Fe}_{1.2}\text{O}_4$	650.7	641.0	625.0

3.10 (b) SATURATION MAGNETISATION STUDY :

For the measurement of saturation magnetisation high field loop tracer designed by C.R.K. Murthy at T.I.F.R. Bombay was used. The instrument consists of an electromagnet working at 50Hz main supply. It produces a sinusoidal field of maximum peak value of 3500 overstead in the air gap of about 9 mm. A special balancing coil is used to deflect the magnetisation of the sample placed in the air gap. The experimental set up is shown in Fig. 3.3.

The signal from the balancing coil after integration has been fed to vertical plates of an oscilloscope after suitable amplification. A signal is proportional to magnetic field which is fed to the horizontal plates of the oscilloscope. Thus the oscilloscope displays magnetic moment against the field i.e. hysteresis loop for the sample. The vertical deflection has been calibrated in terms of magnetic moment in e.m.u. and horizontal deflection in oe/div. The calibration was done with the nickel strip having magnetisation 53.54 e.m.u/gm.

With the help of current upto 100 mA an ellipse on the screen was obtained. For an appropriate size horizontal gain potentiometer were adjusted. Then the ellipse was converted into a straight line by adjusting the vertical phase control. Now by varying 'course' amplitude potentiometer phase difference was confirmed and which was made zero by adjusting horizontal phase potentiometer. The measurement of ' M_g ' value were carried out directly from the C.R.O. screen which was properly illuminated and calibrated before introducing the sample in the core. After introducing the



Fig: 3.3

sample, the set up was once again tested.

The current was gradually increased and hysteresis loop was obtained on the screen of the C.R.O. The division of the C.R.O. on y-axis (magnetisation axis) were calibrated by using standard 'Ni' strip. For the measurement of 'MS' by hysteresis loop on C.R.O. screen, a digital multimeter was connected across the vertical deflection of C.R.O. and reading in milivolts was noted for every ferrite sample and also for standard Ni-sample.

The magnetisation of the series $\text{Cd}_{0.3} \text{Ni}_{0.7+t} \text{Mn}_t \text{Fe}_{2-2t} \text{O}_4$ was calculated as follows.

Example : The standard 'Ni' strip of mass 1.0611 gm displayed the hysteresis loop/ ^{of} effective length 1.6 division. The magnetisation of standard Ni strip is 53.34 emu/gm was used to obtained e.m.u/gram of the sample as,

$$\begin{aligned} \text{Total e.m.u.} &= 53.34 \times \text{weight of standard Ni} \\ &= 56.599 \text{ e.m.u.} \quad \dots\dots(3.19) \end{aligned}$$

Now height 1.6 corresponds to 56.599 emu/gram Therefore height 1 corresponds to 35.374 emu/gram.

Example : The saturation magnetisation 'MS' can be determined as,

$$\begin{aligned} \text{MS} &= 35.374 \times \text{height of sample/weight of sample} \quad \dots\dots(3.20) \\ &= 35.374 \times 2.0 / 1.577 = 44.863 \text{ emu/gm} \end{aligned}$$

similarly ' M_s ' was calculated for other samples.

The measurement of saturation magnetisation (MS) provides saturation magnetic moment ' n_B ' in Bohr magnton can be estimated by,

$$n_B = M_s \times \text{molecular weight} / 5585 \times d_s \quad \dots\dots(3.21)$$

where d_s is density of sample.

3.10 (c) PERMEABILITY :

3.10 (c-1) VARIATION WITH TEMPERATURE :

For the determination of permeability, toroid sample was made with the help of die having inner diameter of 0.85 cm and outer diameter of 1.55 cm, fabricated in this department. An insulated Cu-wire was wound on toroid sample so as to form the core. With the help of Autocompute L-C-R 'Q' meter the values of Q-factor and inductance are noted with different values of temperature at the test frequency of 1 KHz. The reading was noted at an interval of about 20⁰C from room temperature to 600⁰C. The permeability was then calculated by using the relation,

$$L = 0.0046 \quad \mu N^2 h \log_{10} OD/ID \quad \dots\dots(3.22)$$

where L - Inductance in μH

N - number of turns of Cu-wire on toroid

μ - permeability of the core.

h = Thickness of toroid sample in inches.

OD - outer diameter in inches.

ID - Inner diameter in inches.

3.10.(c-2) VARIATION WITH FREQUENCY :

Impedance analyser of the frequency range 5Hz to 13MHz (Hewlett- Paackard model- 4192A) was used to measure inductance and quality factor at. E.T.D.C. Bangalore. All the measurements were done at room temperature. For this measurements, all the samples are in the form of toroids. Initially the instrument was set for lower frequency to obtain steady values of inductance L and $\tan \delta$ i.e. factor D. The working voltage of the instrument was kept constant i.e. 0.7 volt. Then the inductance values were scanned from 2KHz to 4MHz and readings were noted for successive steps. The initial permeability for corresponding frequencies was calculated by using the relation (3.22).

3.11 RESULTS AND DISCUSSION :

3.11(a) MAGNETISATION :

In the Table 3.2 the values of magnetisation, magnetic moment, porosity are given.

The observed magnetic moment for $\text{Cd}_{0.3}\text{Ni}_{0.7}\text{Fe}_2\text{O}_4$ agree well with the reported value. It is observed that the magnetic moment of all the samples decrease with increasing Mn^{4+} content. The magnetisation behaviour has been studied on the basis of cation distribution. A.R. Das³⁰ et al have studied the effect of the tetravalent substitutents like Ti, Zr, Sn on magnetisation in Ni-Zn ferrites, S.R.Jadhav³¹ et al in Cu-Zn ferrites. The general for cation distribution is,

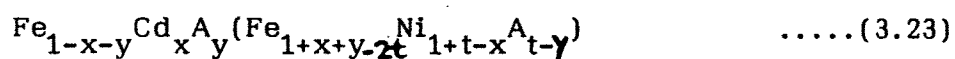
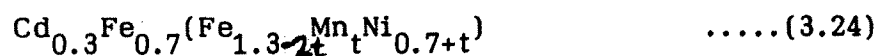


TABLE 3.2
VALUES OF MAGNETISATION, DENSITY, MAGNETIC MOMENT AND
POROSITY

Composition	Ms emu/gram	densities gm/cc	n_B Bohr magneton calculated	Porosity
$Cd_{0.3}Ni_{0.7}Fe_2O_4$	44.863	4.068	3.957	25.975
$Cd_{0.3}Ni_{0.75}Mn_{0.05}Fe_{1.9}O_4$	43.944	4.421	3.568	20.039
$Cd_{0.3}Ni_{0.8}Mn_{0.1}Fe_{1.8}O_4$	47.185	4.386	3.863	20.589
$Cd_{0.3}Ni_{0.85}Mn_{0.15}Fe_{1.7}O_4$	43.404	4.171	3.739	-
$Cd_{0.3}Ni_{0.9}Mn_{0.2}Fe_{1.6}O_4$	43.281	4.342	3.582	21.468
$Cd_{0.3}Ni_{1.0}Mn_{0.3}Fe_{1.4}O_4$	35.619	4.119	3.110	25.329
$Cd_{0.3}Ni_{1.1}Mn_{0.4}Fe_{1.2}O_4$	30.130	4.052	2.677	-

where A- tetravalent ion like Ti, Mn, Zr, Sn etc.

Gorter³² has classified cations into different groups on the basis of electronic configuration. According to his classification, the transition metal ions with $3d^3$ and $3d^8$ configurations prefer B-sites. These configuration belongs to Mn^{4+} and Ni^{2+} ions. Metal ion distribution in the system of $Mn_xFe_{3-x}O_4$ ($1 < x < 2$) was studied with the help of neutron diffraction experiment and it is suggested that Mn^{2+} goes to A-site whereas Mn^{3+} and Mn^{4+} prefer B-sites. Considering the above facts the cation distribution for our system $Cd_{0.3}Ni_{0.7+t}Mn_tFe_{2-2t}O_4$ can be written as,



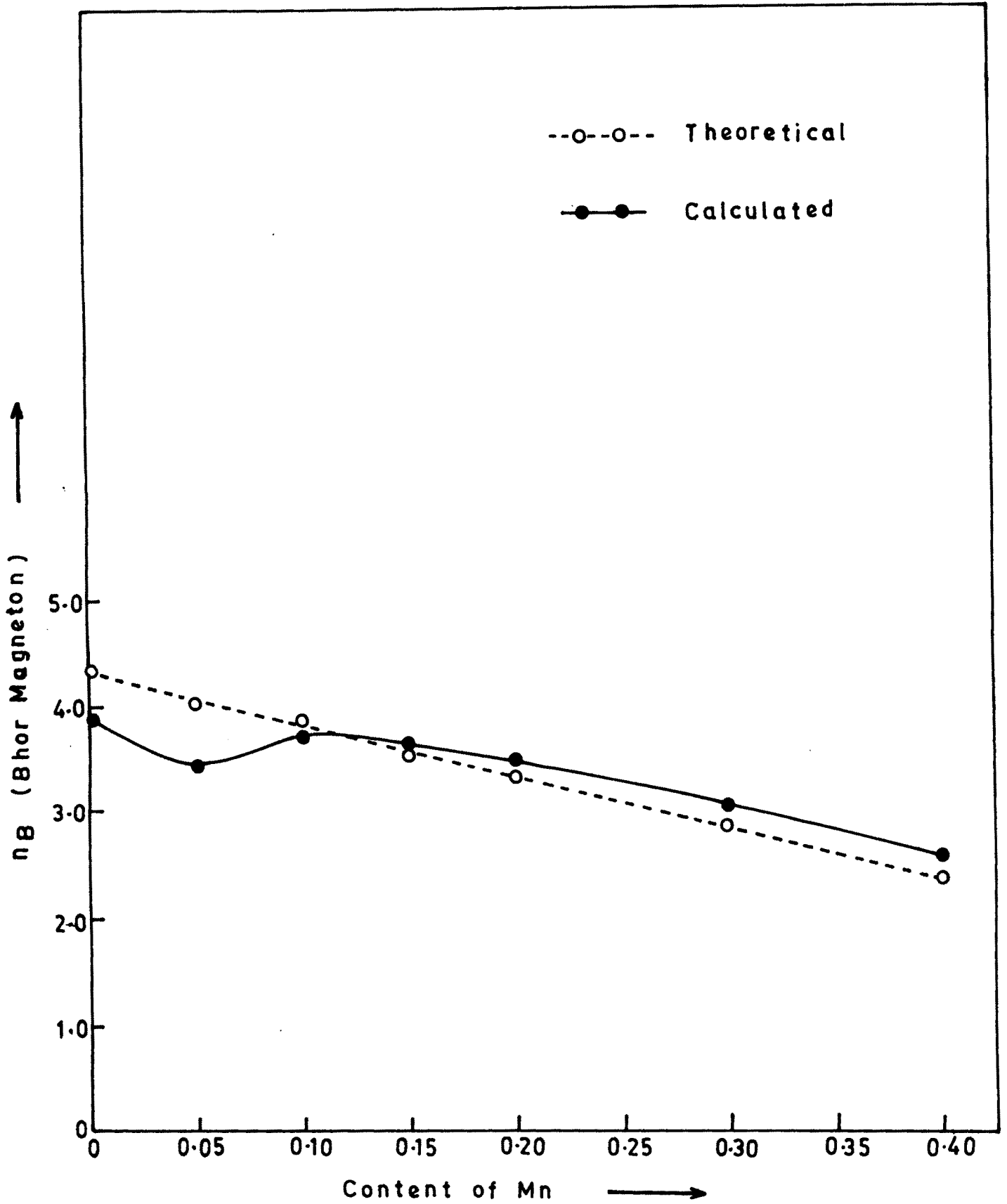
where t varies between 0 to 0.4.

The magnetisation of the ferrite compositions are estimated on the basis of Neel molecular field model. According to this model the A-B interaction is stronger than B-B and A-A interactions. The net magnetisation is the vector sum of magnetisations of octahedral (B) and tetrahedral (A) sites ($M_0 = M_B - M_A$). In this model collinear arrangement of magnetic moments of the individual sites is presumed i.e. magnetic ions on each sub-lattice are ferromagnetically aligned.³³ The cation distribution and magnetic moments (calculated and theoretical) are given in Table 3.3.

TABLE 3.3
VALUES OF MAGNETIC MOMENT

Cation distribution	Magnetic moment in Bohr magneton	
	Calculated	Theoretical
$\text{Cd}_{0.3}\text{Fe}_{0.7}(\text{Ni}_{0.7}\text{Fe}_{1.3})$	3.957	4.40
$\text{Cd}_{0.3}\text{Fe}_{0.7}(\text{Ni}_{0.75}\text{Mn}_{0.05}\text{Fe}_{1.2})$	3.568	4.15
$\text{Cd}_{0.3}\text{Fe}_{0.7}(\text{Ni}_{0.8}\text{Mn}_{0.1}\text{Fe}_{1.1})$	3.863	3.90
$\text{Cd}_{0.3}\text{Fe}_{0.7}(\text{Ni}_{0.85}\text{Mn}_{0.15}\text{Fe}_{1.0})$	3.739	3.65
$\text{Cd}_{0.3}\text{Fe}_{0.7}(\text{Ni}_{0.9}\text{Mn}_{0.2}\text{Fe}_{0.9})$	3.582	3.40
$\text{Cd}_{0.3}\text{Fe}_{0.7}(\text{Ni}_{1.0}\text{Mn}_{0.3}\text{Fe}_{0.7})$	3.110	2.90
$\text{Cd}_{0.3}\text{Fe}_{0.7}(\text{Ni}_{1.1}\text{Mn}_{0.4}\text{Fe}_{0.5})$	2.677	2.40

These values agree well with the observed result. The slight increase of 'nB' (calculated), for the composition of $t = 0.1$ may be due to superparamagnetic behaviour of Fe^{3+} ions in the system. The variation of magnetic moment with content of Mn is also shown in Fig. 3.4.

FIG. 3-4 — VARIATION OF η_B WITH CONTENT OF Mn.

Similar behaviour have been observed by S.A.Patil³⁴ et al for Ti substituted Mg ferrites. It is observed that the magnetisation decreases continuously with Ti upto 0.4 content and shows an increase at 0.4 and then decreases. P.Kishan et al³⁵ have studied the magnetic properties of Ti substituted Li ferrite by Mossbour spectroscopy. They have observed a small increase in the hyperfine field at $t = 0.4$ and suggested that the Fe^{3+} ion is responsible for the appearance of superparamagnetic doublet contributing to hyperfine fields.

The total magnetisation is also dependent on the grain size, porosity and impurity phases. The presence of pore impedes the motion of domain walls. This reduces the magnetisation with increase of porosity. When crystallites are large with negligible porosity crystalline anisotropy reduces making magnetisation easy. The effect of porosity, density on magnetisation in normal and hot pressed Mn-Zn-Ni ferrites by R.K. Puri³⁶ et al and reported that the hot pressed ferrite shows higher magnetisation than the normal. Such behaviour can only be observed with electron microscope and chemical analysis. The porosity in present system increases with Mn^{4+} , hence the magnetisation decreases.

3.11 (b) CURIE TEMPERATURE :

The Curie temperature decreases continuously with increase of Mn^{4+} ions. The observed Curie temperature, calculated Curie temperature from permeability and conductivity experiment are shown

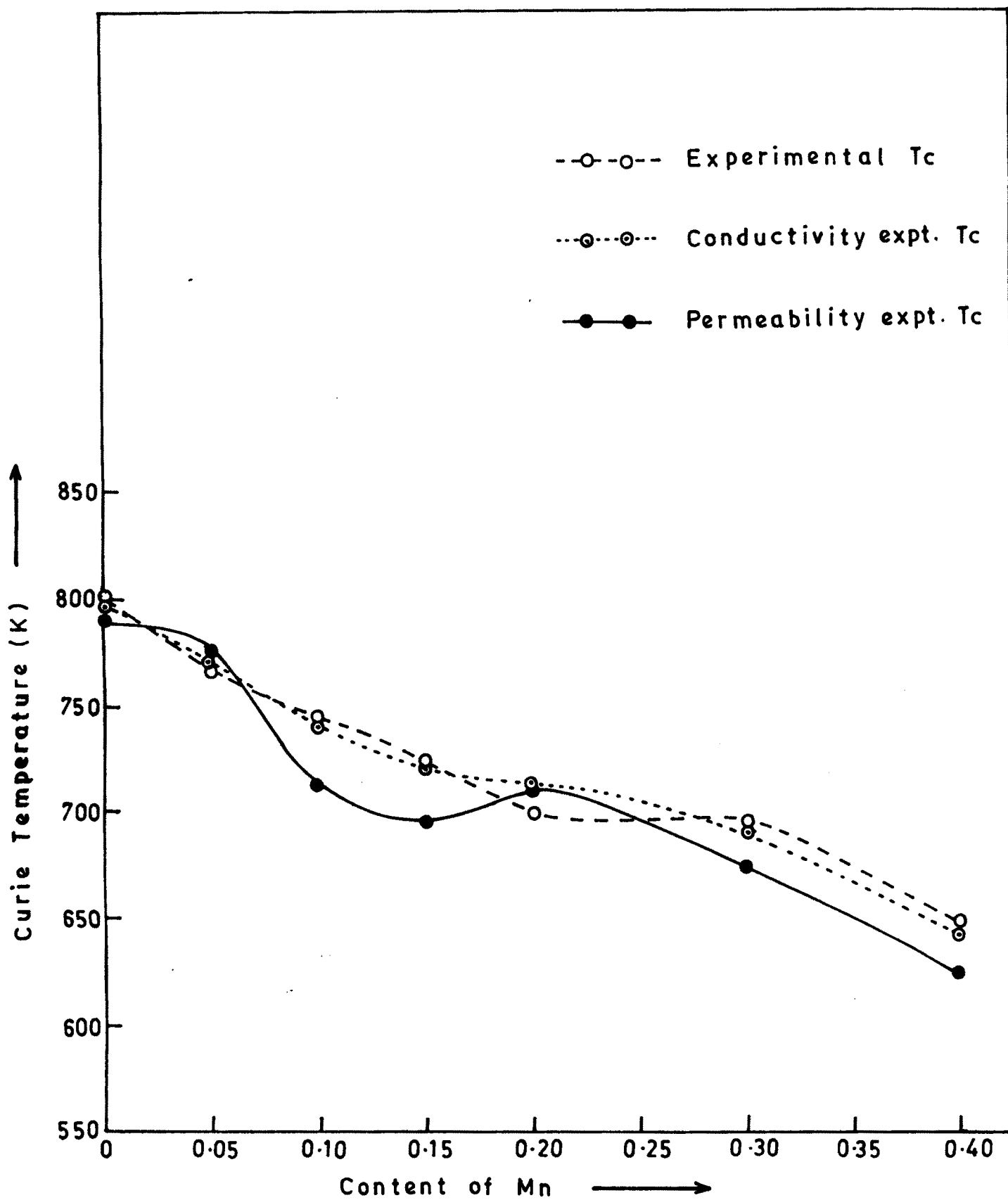
in Fig. 3.5 which shows similar behaviour with small variation in values. The number of workers studied the behaviour of Curie temperature with substitution of tetravalent ions by replacing Fe^{3+} ions.³³ They found that 'Tc' decreases linearly as the concentration of tetravalent ion increase. The decrease in Tc is due to decrease in A-B interaction energy and total number of A-B interactions in the system.

3.11(c) PERMEABILITY :

Variation of initial permeability with temperature for the samples Cd_1 to Cd_7 is shown in Fig. 3.6. From these figures the following observations have been made.

1. Room temperature permeability decreases considerably on the addition of Mn^{4+} . All these samples also shows decrease of Curie temperature. The permeability is maximum for $t = 0$.
2. For the samples with $t = 0$ the ' μ_i ' slowly increases upto the temperature 500°K , and then decreases and becomes very small at the temperature 778°K , which is nearly equal to the Curie temperature of the sample.
3. The effect of addition of Mn^{4+} is to make ' μ_i ' almost invariant with temperature and suppresses the peaking behaviour.

The density of the sample influence bulk magnetic properties. The observed decrease in permeability can therefore be attributed to decrease of density of the samples on addition of Mn^{4+} . Similar

FIG. 3-5 - VARIATION OF T_c WITH CONTENT OF Mn .

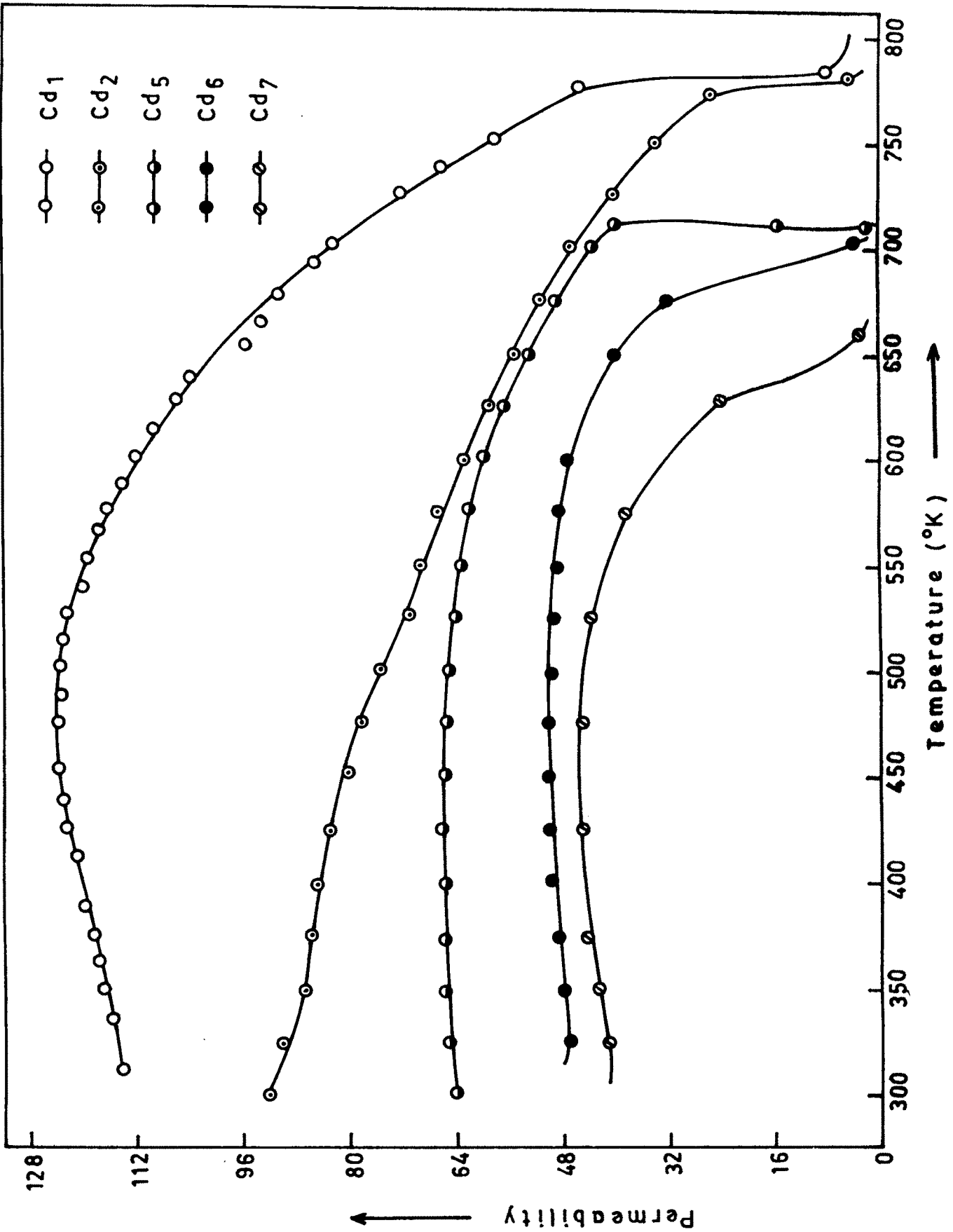


FIG. 3-6 — VARIATION OF INITIAL PERMEABILITY WITH TEMPERATURE .

results have been obtained in 'Zr' substituted Cu-Zn ferrites³¹ Fomenov and Bashikieve observed the increase in ' μ_i ' on addition of Ti for Mn-Zn ferrites³⁷ which they attributed to compensation of an anisotropy constant which appears when ferric ions are replaced according to the formula.



On replacing 'Zr' and 'HF' a decrease in μ_i is observed over the whole temperature region investigated by them. According to them, the 'Zr' and HF cations do not have the same effect on the anisotropy constant as the 'Ti' cations. However, in Mn^{4+} substitution similar type of effect leading the reaction.



appears to be unlikely. Hence there is no increase in ' μ_i ' on Mn^{4+} addition. The Curie temperature decreases contineously with Mn^{4+}

Fig. 3.7, 3.8 shows μ_i and $\tan \delta$ with frequency respectively. From this plot the following observations can be made.

1. Initial permeability decreases with frequency upto 10 KHz and remains constant upto 1 MHz and suddenly increases at and above frequencies.
2. The permeability observed at 10 KHz decreases with increase of Mn^{4+} containt.
3. All the samples show similar behaviour with frequency variation of permeability.

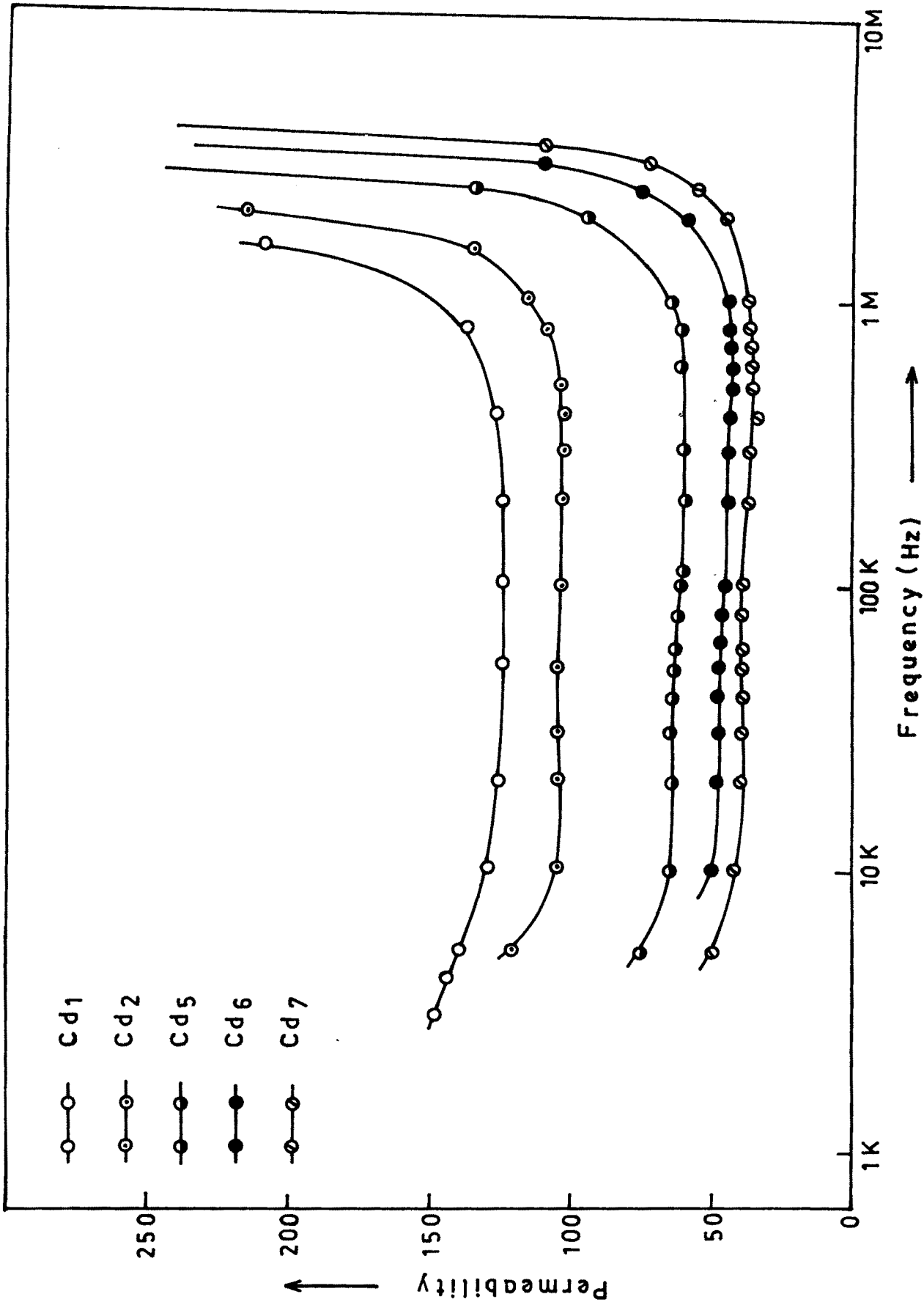


FIG.3-7 — VARIATION OF PERMEABILITY WITH FREQUENCY .

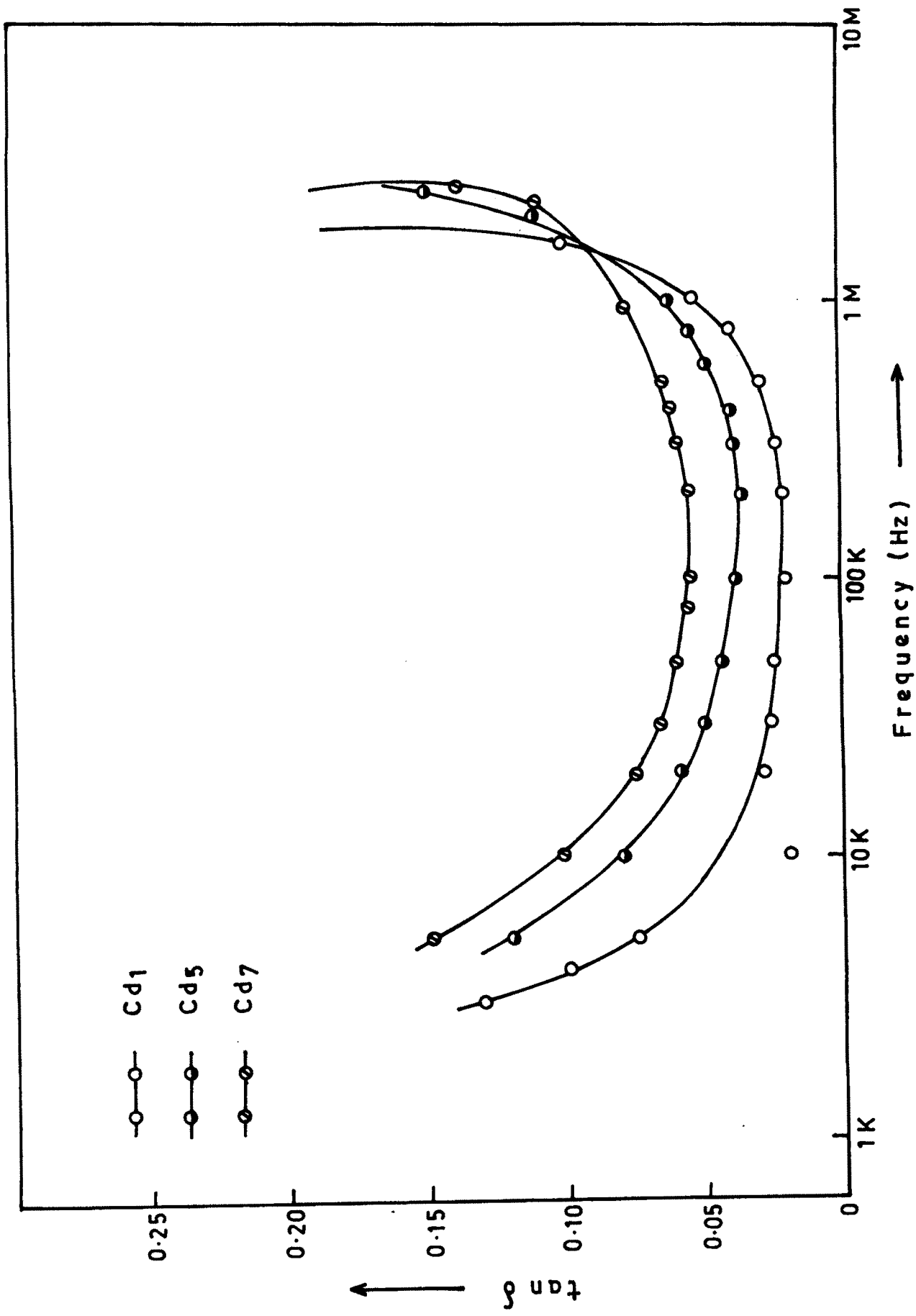


FIG. 3-8 — VARIATION OF $\tan \delta$ WITH FREQUENCY .

The physical mechanism contributing to the initial magnetic permeability ' μ_i ' are, rotation of magnetisation and displacement of domain walls. Both these contributions are related to ' k_i ' and saturation magnetisation. Rado and Terris³⁸ observed low frequency dispersion in ferrites which they attributed to domain wall displacement. The absence of low frequency resonance indicate the absence of domain wall movements. The initial permeability (μ_i) also depends on the method of preparation and its value changes markedly with firing temperature, if the heat treatment modulates in the porosity. Similar losses have been observed in Cu-containing ferrites.

In the case of polycrystalline ferrite with a low frequency permeability of comparable magnitude μ' and μ'' are only weakly dependent on frequency upto MHz region.

Considering the above facts, it can be concluded that the addition of Mn^{4+} hinders the domain wall motion and domain wall displacement and makes μ_i' almost frequency independent. The sudden increase in permeability at and above 1 MHz in our samples may be due to change in grain size. Buck and Ross³⁹ have found that, when the grain size of polycrystalline Mn-Zn ferrite is increased, the frequency dependence of ' μ_i' ' and μ'' at frequencies well below the resonance frequency. increases suddenly.

Globus⁴⁰ has given the following approximate relation as

$$\mu_i = M_s^2 d m / K_1 \quad \dots\dots(3.26)$$

where K_1 = is anisotropy constant

M_s = is saturation magnetisation

d_m = is grain diameter.

Since the addition of Mn^{4+} decreases the value of ' M_s ', and if grain size does not change significantly and K_1 remains invariant, ' μ_i ' decreases. Thus the variation of $\mu_i(T)$ and $\mu_i(f)$, Mn^{4+} contributes much in changing the nature of permeability spectrum. The higher concentration of Mn^{4+} is expected to modify the microstructure, grain growth, density, which are influencing factors to the permeability behaviour. However, the decrease in ' μ_i ' with addition of Mn^{4+} can be explained only with the knowledge of anisotropy constant.

REFERENCES

1. Neel L., 'Magnetic properties of ferrites, ferrimagnetism and antiferrimagnetism' Ann. Physique 3, 137 (1948)
2. C.M. Srivastava, M.J. Patani and T.T. Srnivasan., J.Appl. Phys.53(3), P. 2107 (1982).
3. A.M. Alper, 'High temperature oxides' Academic Press, N.Y. (1971).
4. E.Sterm, J.Appl. Phys. Vol. 38, No.3, P.1397-99 (1967).
5. L.F. Bates, Modern Magnetism C.V.F.P. 5 (1951).
6. D.O. Smith, Rev. Sci. Instr. 27, P. 261 (1965).
7. D.Fidman and R.P. Hunt, Z-Instrument Kunde 27, P. 259 (1964).
8. S.Fener, Rev. Sci. Instr 27, P 584 (1956).
9. S.Fener, and E.J. Mic., Nife, Rev. Sci. Instr 39, P. 171, (1968).
10. C.Kittle, Phys. Review 73, P-155. (1948).
11. H.Brand and H.W. Fieweger, Proc. IEEE 53, P. 186 (1965).
12. Weiss P. J., De Phisique 6, 661 (1907).
13. Barkhausen H., Phys. Zeits 20, 401 (1919).
14. Heisenberg W., Zeit Fur Phys. 49, 619 (1928).
15. Stonner E.C., Phil. Mag. 15, 1018 (1933).
16. Lux and Button, 'Microwave ferrites and ferrimagnetism' Mc Grawhill Book Company Inc . P-4, (1962).
17. Y.Yafet and C.Kittle, Phys. Rev. Vol. 87, P. 290 (1952).
18. J.Kanamen , in 'Magnetism' G.I. Radio and Shull. C.G., edi. Academic Press. N.7., P-127, (1963).

19. Zener C., Phys. Rev. 96, 1335 (1954).
20. Bloch F., Zeit Fur Phys. 74, 295 (1932).
21. Kondorsky E., Phys. Z. Sowjetunion, 11, 597 (1937)
22. Keroten M., Grundlagen Ciner Theorie der ferromagnetischem. Hysteresese under Kuerzihvloraft Hirzel Leipzig (1943).
23. A. Goral and H. Wierzba, Bull-Acad Pol Sci. Ser. Sci. Tech. 12, 91 (1964).
24. A Globus, J. Phys. (paris) C-I, 1 (1977).
25. G. Buttino, A Cechetti and A. Drigo., IEEE. Trans Magn, 2, 430 (1966).
26. G. Buttino., A. Cechetti, M. Poppi and G. Zini, Presented at 3rd Joint Intermag-Magnetism and magnetic material, menfreal, quebec, Canada (1982).
27. E. Schloemann., J. Appl. Phys. Vol. 41, P 204-214 (1970).
28. E. Schloemann, J. Appl. Phy. Vol. 32, PP 443-451 (1971).
29. E.C. Snelling, Ferrite for linear applications IEEE spectrum January 46, (1972).
30. A.R. Das, V.s. Ananthan and D.C. Khan, J. Appl. Phys. 57a, (15th April 1985).
31. S.R. Jadhav, S.R. Sawant, S.S. Suryavanshi, S.A. Patil, R.N. Patil, ICF-5, India P-453, (1989).
32. Gorter E.W., Philips. Res. Rep. Vol-9, 295 (1954).
33. D.R. Sagar, Chandra Prakash, S.N. Chatterjee and Pran Kishan, Proc. ICF-5, 441. India (1989).
34. S.A. Patil, C.N. Jadhav, S.S. Suryavanshi, S.R. Sawant, R.N. Patil, ICEM-90, Sept 17-19, 1990 Newark New Jersey, USA.

35. P.Kishan, C.Prakash, J.S.Baijal, K.K. Laroia, Phy. Stats. Sol(a) 84, 535 (1984).
36. R.K.Puri, Vijay K.Babbar, R.G. Mendiratta, Proc. ICF-5, 239-243, (1989).
37. Fomenko, G.V. and Bashkriov L.A., Izvestiya Akademi Nauk, SSSR Neogranicheskia Materaly Vol.38, 11.P-1886,(1982).
38. Rado J.T. and Terris, Phys. Rev. 83, 177 (1951).
39. Buck and Ross, Phys. Stats Solidi 32, 659 (1969).
40. Globus A., et al IEEE Trans, on mag-mag-7, 617 (1971).